Isozaki *NPG Asia Materials* (2026)18:9
https://doi.org/10.1038/s41427-026-00636-9

NPG Asia Materials

REVIEW ARTICLE Open Access

Superatomic molecules: natural and non-natural atom-like bonding between superatoms

Katsuhiro Isozaki[1,2]

Abstract

Superatomic molecules, formed by the fusion or combination of spherical metal nanoclusters (superatoms), have emerged as a novel framework for understanding the stability of anisotropic metal nanoclusters. Advances in the synthesis and structural characterization of these anisotropic clusters have provided valuable insights into the classification of superatomic molecules and the development of a corresponding bonding theory. This review offers a qualitative perspective on the relationship between molecular geometry and electronic structure in superatomic molecules, focusing on superatomic molecular orbitals formed through the linear combination of individual superatomic orbitals—analogous to atomic orbitals in natural molecules. Unique stabilization features, not observed in conventional molecular systems, are also highlighted. Furthermore, the review discusses potential functional properties of superatomic molecules in the context of future applications.

Introduction

Ligand-protected metal nanoclusters, especially those based on gold, have attracted considerable attention due to their potential applications in catalysis and photofunctional materials[1–12]. Extensive research on their structural determination and electronic properties has revealed that these nanoclusters are stabilized by forming discrete electron shells that accommodate valence electrons. This behavior can be described by "Jellium model"[13]. Because their electron configurations resemble Bohr's atomic model, such nanoclusters are often referred to as "superatom"[14].

Most metal nanoclusters possess spherical geometries, and their electronic structures can be well explained by superatom theory. However, there also exist non-spherical, anisotropic metal nanoclusters—often called "cluster of clusters"[15]—whose stability cannot be accounted for by the simple Jellium model. To explain the stability of these structures, Cheng and Yang proposed the super valence bond (SVB) theory[16–18]. In this theory, the stability arises from the formation of superatomic molecular orbitals (SAMOs), and such clusters are referred to as "superatomic molecules" (Fig. 1). These molecules are formed by the linear combination of superatomic orbitals (SAOs), in a manner analogous to how natural atoms form molecular orbitals through the combination of atomic orbitals.

Although superatomic molecules exhibit natural atom-like bonding schemes, some of them display unique features that deviate from those observed in natural atomic systems—there are considered characteristic traits of superatomic molecules. This review introduces the concept of superatoms, presents representative examples, highlights recent advances, and discuss future perspective on the development and application of superatomic molecules.

What is superatom?

"Superatom" represents a cluster composed of several atoms that collectively behave like a single atom, particularly due to the stabilization arising from the closure of electronic shells. Early studies using ultraviolet photoelectron spectroscopy (UPS) of gas-phase clusters such as Au_n^-, Ag_n^-, and Cu_n^- revealed that their electron affinities drop sharply at specific "magic numbers" (e.g., $n = 8$, 20, 34, and 58)[19]. According to the jellium model[13], the stability of these coinage metal clusters can be explained by the closure of superatomic electron shells. In this model, valence electrons are delocalized and confined in quantized orbitals, so-called "superatomic orbitals"

Correspondence: Katsuhiro Isozaki (kisozaki@scl.kyoto-u.ac.jp)
[1]Institute for Chemical Research, Kyoto University, Kyoto, Japan
[2]Graduate School of Engineering, Kyoto University, Kyoto, Japan

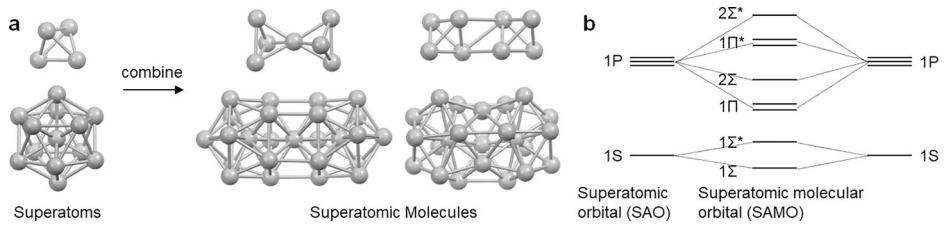

Fig. 1 Concept of superatomic molecules. a General scheme for the formation of superatomic molecules by the combination of superatoms. **b** Energy diagram of the formation of superatomic molecular orbitals by the combination of superatomic orbitals.

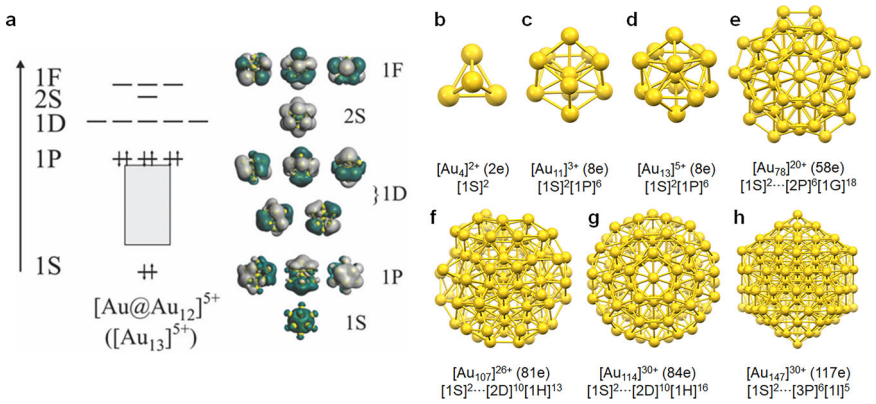

Fig. 2 Examples of spherical gold superatoms. a Energy diagram and SAOs of $[Au_{13}]^{5+}$ superatom. The formula with charge state (the number of valence electrons in parenthesis), and its electron configuration in superatomic orbitals, 1S, 1 P, 1D, etc of **b** $[Au_4]^{2+}$, **c** $[Au_{11}]^{3+}$, **d** $[Au_{13}]^{5+}$, **e** $[Au_{78}]^{20+}$, **f** $[Au_{107}]^{26+}$, **g** $[Au_{114}]^{30+}$, and **h** $[Au_{147}]^{30+}$. **a** Reproduced with permission from Royal Society of Chemistry[23].

such as 1S, 1 P, 1D, 2S, 1 F, 2 P, 1 G, and so on, analogous to atomic orbitals. The magic numbers (n = 2, 8, 18, 20, 34, 40, 58, etc) correspond to fully filled superatomic shells, contributing to cluster stability.

This superatomic behavior is not limited to gas-phase clusters. Similar shell-closing characteristics are also observed in ligand-protected coinage metal clusters. Since the discovery of thiolate-protected gold nanoclusters[1,2], a wide variety of ligand-protected gold nanoclusters have been synthesized, incorporating different numbers of gold atoms and several types of ligands, such as thiolate[20–22], alkynyl[10], amide[11], phosphine, N-heterocyclic carbene (NHC)[12], etc. In most cases, the gold atoms form a superatomic core. However, in thiolate- and alkynyl-protected clusters, the core is further stabilized by gold–ligand oligomers known as staples.

Several representative gold superatoms have been reported, such as $[Au_4]^{2+}$, $[Au_{11}]^{3+}$, $[Au_{13}]^{5+}$[23], $[Au_{78}]^{20+}$, $[Au_{107}]^{26+}$, $[Au_{114}]^{30+}$, and $[Au_{147}]^{30+}$ (Fig. 2)[4,24]. Their valence electron counts, 2e, 8e, 8e, 58e, 81e, 84e, and 117e, respectively, mostly correspond to the magic numbers identified in gas-phase UPS studies. The electron configurations of these superatoms can be described in terms of SAOs, such as $(1S)^2$, $(1S)^2(1\,P)^6$, $(1S)^2(1\,P)^6$, $(1S)^2....(2\,P)^6(1\,G)^{18}$, $(1S)^2....(2D)^{10}(1H)^{13}$, $(1S)^2....(2D)^{10}(1H)^{16}$, and $(1S)^2....(3\,P)^6(1\,I)^5$, with most exhibiting closed electronic shells. Owing to their closed-shell nature, $[Au_4]^{2+}$ and $[Au_{11}]^{3+}/[Au_{13}]^{5+}$ are regarded to helium- and neon-type superatoms, respectively.

Similar ligand-protected silver superatoms have also been identified, including $[Ag_{13}]^{5+}$ (8e)[25], $[Ag_{32}]^{14+}$ (18e), $[Ag_{28}]^{8+}$ (20e)[26], $[Ag_{38}]^{18+}$ (20e), and $[Ag_{103}]^{45+}$ (58e).[4] Recently, a copper-based spherical superatom, $[Cu_{13}]^{5+}$ (8e), was also reported by Sun[27].

All of these superatoms have the potential to act as building block for superatomic molecules by the combination with other superatoms.

Superatomic molecules with natural atom-like bonding

The concept of superatomic molecules was first introduced by Cheng and Yang in 2013[16–18], who proposed the super valence bond (SVB) theory to describe the bonding interactions between superatoms through the formation of superatomic molecular orbitals (SAMOs). Within this theoretical framework, the $Au_{38}(SR)_{24}$ nanocluster[28,29], possessing a $[Au_{23}]^{9+}$ core, was identified as an F_2-type superatomic molecule[16]. Density functional theory (DFT) calculations demonstrated the formation of SAMOs, designated as Σ, Σ*, Π, and Π*, via the linear combination of constituent SAOs.

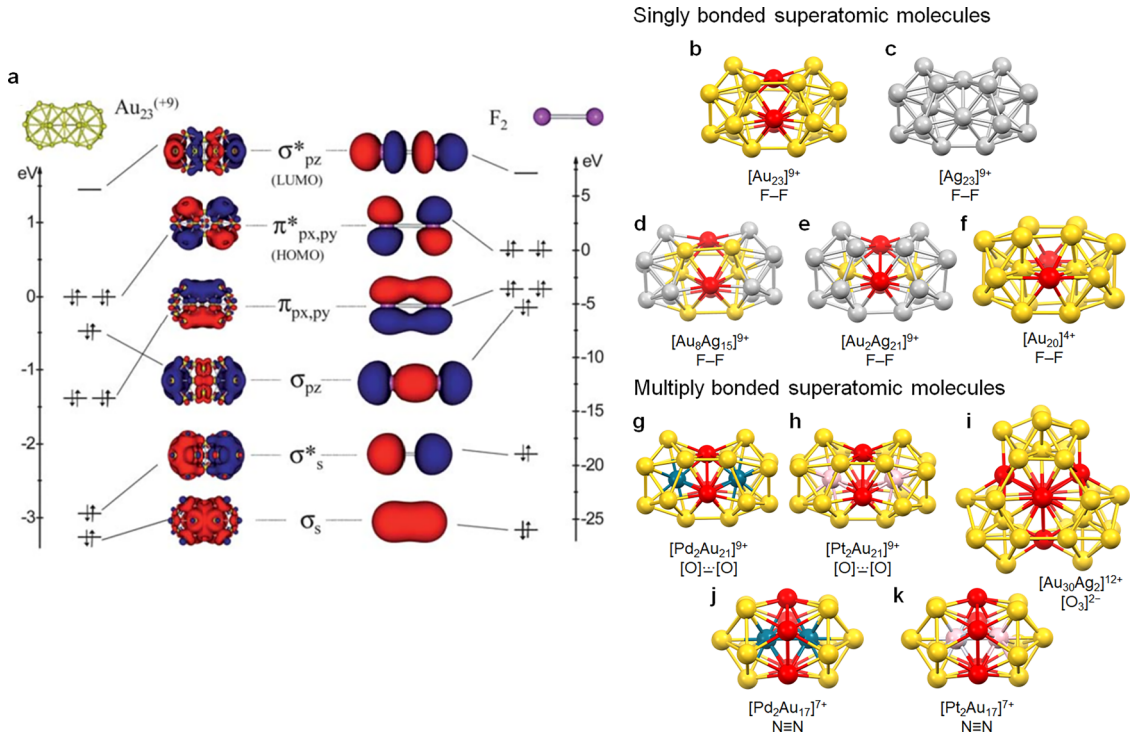

Fig. 3 Examples of superatomic molecules with natural atom-like bonding. a Superatomic molecular orbitals in the F_2-type superatomic molecule with $[Au_{23}]^{9+}$ core. Singly bonded superatomic molecules: **b** $[Au_{23}]^{9+}$, **c** $[Ag_{23}]^{9+}$, **d** $[Au_8Ag_{15}]^{9+}$, **e** $[Au_2Ag_{21}]^{9+}$, **f** $[Au_{20}]^{4+}$. Multiply bonded superatomic molecules: **g** $[Pd_2Au_{21}]^{9+}$, **h** $[Pt_2Au_{21}]^{9+}$, **i** $[Au_{30}Ag_2]^{12+}$, **j** $[Pd_2Au_{17}]^{7+}$, **k** $[Pt_2Au_{17}]^{7+}$. Color code, yellow: gold, gray: silver, green: palladium, pink: platinum, red: shared gold/silver atom. **a** Reproduced with permission from Royal Society of Chemistry[16].

Fourteen valence electrons are accommodated within these SAMOs in the electron configuration of $(\Sigma)^2(\Sigma^*)^2(\Pi_{px,py})^4(\Sigma_{pz})^2(\Pi^*_{px,py})^4$, corresponding to a singly bonded structure analogous to that of the diatomic F_2 molecule (Fig. 3a)[30]. The $Au_{38}(SR)_{24}$ nanoclusters are the pioneering superatomic molecule and the $[Au_{23}]^{9+}$ core exhibits inherent chirality, thus their catalytic[31–35] and chir-optical[36–38] properties have been extensively studied to date.

This bonding scheme suggests that two Au_{13} (7e, F-type) superatoms are fused through the sharing of three gold atoms and two electrons, resulting in an F_2-type superatomic molecule (Fig. 3b). Analogous structural motifs have also been reported in silver and gold–silver alloy nanoclusters, including $[Ag_{23}]^{9+}$[39], $[Au_8Ag_{15}]^{9+}$, and $[Au_2Ag_{21}]^{9+}$[40], all of which have been categorized as F_2-type superatomic molecules (Fig. 3c–e).

Furthermore, Cheng and Yang identified $Au_{20}(PPh\text{-}Py_2)_{10}Cl_4]Cl_2$ nanocluster bearing a $[Au_{20}]^{6+}$ core as another F_2-type superatomic molecule (Fig. 3f)[17]. In this case, two Au_{11} (7e, F-type) superatoms are joined by sharing two gold atoms and two electrons. Similarly, Tsukuda proposed that $Au_{25}(SDpp)_{11}$, synthesized via thiolation of a polyvinylpyrrolidone-stabilized gold nanocluster, also adopts an F_2-type superatomic molecular structure[41].

All these F_2-type superatomic molecules exhibit single superatomic bonding, with the electron configuration $(\Sigma)^2(\Sigma^*)^2(\Pi_{px,py})^4(\Sigma_{pz})^2(\Pi^*_{px,py})^4$[4]. The formal bond order of these superatomic molecules can be tuned by electron oxidation and reduction to produce $[F_2]^+$ and $[F_2]^-$[42,43]. Oxidized analogues such as $[Au_{38}(SR)_{24}]^{2+}$ and $[M_2Au_{36}(SR)_{24}]$ (M = Pd, Pt)[44,45], which contain 12 valence electrons, have been postulated to correspond to O_2-type superatomic molecules[30,46,47]. Takano and Tsukuda successfully synthesized $[M_2Au_{36}(SR)_{24}]$ (M = Pd, Pt) nanoclusters by a newly developed fusion reaction between hydride-activated $[MAu_8(PPh_3)_8]^{2+}$ and $[M'Au_{24}(SR)_{18}]^-$[48,49]. Single crystal X-ray diffraction and DFT calculations revealed that the resulting $[M_2Au_{21}]^{9+}$ cores (Fig. 3g, h) adopt an electron configuration of $(1A_1)^2(1B_2)^2(2A_1)^2(3A_1)^2(1B_1)^2(2B_2)^2$ in C_{2v} symmetry, which differs from the $D_{\infty h}$ symmetry of the ideal O_2 molecule. Although this configuration deviates from that of molecular O_2 due to the bent geometry of the two MAu_{12} superatoms, the formal bond order is higher than that observed in singly bond superatomic molecules.

Shi and Cheng subsequently reported another superatomic molecule exhibiting an even higher bond order[50]. DFT calculations suggested the presence of a three superatomic center-two electron (3sc-2e) bond within the

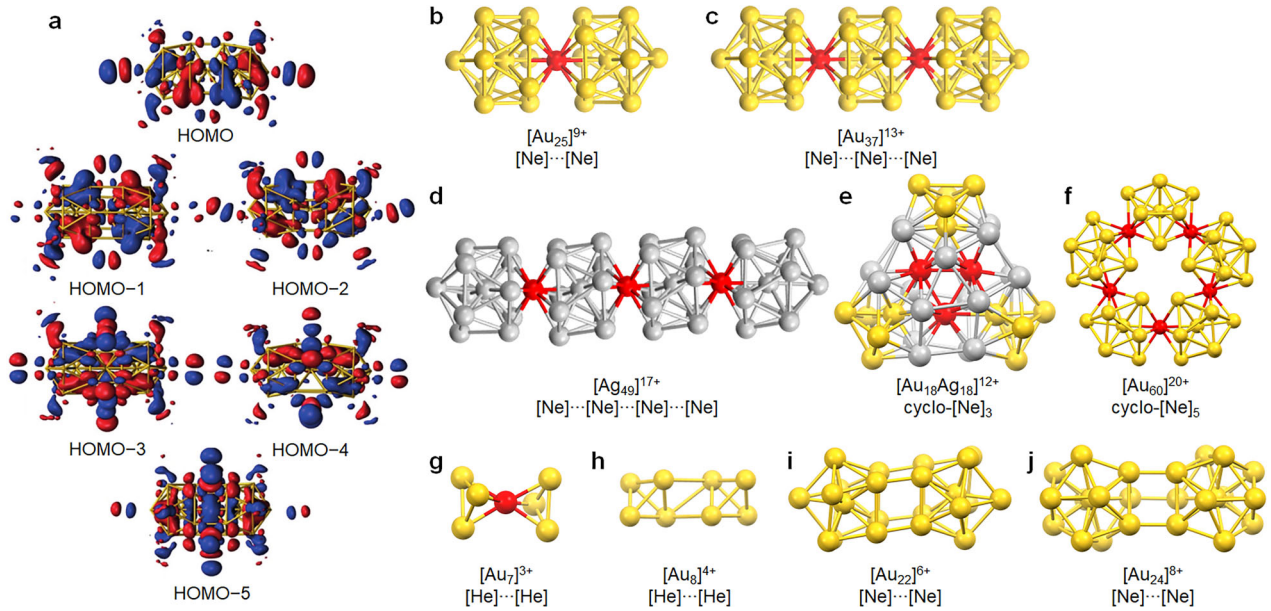

Fig. 4 Examples of superatomic molecules with non-natural atom-like bonding. a Schematic image of filled superatomic molecular orbitals in non-bonding [Ne]···[Ne]-type superatomic molecules. Non-bonding superatomic molecules: **b** $[Au_{25}]^{9+}$, **c** $[Au_{37}]^{13+}$, **d** $[Ag_{49}]^{17+}$, **e** $[Au_{18}Ag_{18}]^{12+}$, **f** $[Au_{60}]^{20+}$, **g** $[Au_7]^{3+}$, **h** $[Au_8]^{4+}$, **i** $[Au_{22}]^{6+}$, **j** $[Au_{24}]^{8+}$. Color code, yellow: gold, gray: silver, red: shared gold/silver atom. **a** Reproduced with permission from Wiley[43].

$[Au_{30}Ag_2]^{12+}$ core of the $Au_{36}Ag_2(SR)_{18}$ nanocluster (Fig. 3i)[51]. In this system, three $Au_{11}Ag_2$ superatoms are arranged in a cyclic manner, with each pair sharing one gold atom and two electrons to form Σ-type 2sc-2e bonds, while the two silver atoms collectively contribute to a central 3sc-2e bond. This bonding motif is analogous to that found in the $[O_3]^{2-}$ ion, leading to the assignment of an $[O_3]^{2-}$-type superatomic molecule.

Although no doubly bonded superatomic molecules have yet been reported, triply bonded superatomic molecules were recently disclosed by Isozaki and Nakamura[52]. A photoinduced fusion reaction between $MAu_{12}(PR_3)Cl_4$ (M = Pd, Pt) clusters led to the formation of N_2-type superatomic molecules, $M_2Au_{17}(PR_3)_{10}Cl_7$ featuring $[M_2Au_{17}]^{7+}$ cores, the first known examples exhibiting superatomic Π-bonding (Fig. 3j, k). Notably, these species display pronounced absorption features attributed to symmetry-allowed electron transition between superatomic molecular Π-orbitals, demonstrating photophysical behavior reminiscent of conventional molecular orbitals.

In addition to the aforementioned synthetic examples, several superatomic molecules featuring natural atom-like bonding have been theoretically predicted. Recently, Cheng demonstrated that sequential or multiple 2sc-2e bonding between metal-doped $M@Au_{12}$ superatoms can give rise to a variety of superatomic analogues of small molecules, including Cl_2, $^1O_2$, $^3O_2$, N_2, CO, CO_2, CF_4, Cl_3^-, O_3, N ≡ C–C ≡ N, and Cl–C ≡ C–Cl[53,54].

Superatomic molecules with non-natural atom-like bonding

In addition to exhibiting natural atom-like bonding behavior, superatomic molecules can also display non-natural bonding characteristics, in which multiple superatoms are connected through formally non-bonding interactions in the absence of direct electron sharing. Under ambient conditions, noble gas atoms are generally inert and do not form chemical bonds. However, numerous superatomic molecules have been reported that structurally resemble non-bonded dimers, trimers, or oligomers of noble gas-type superatoms, such as [He]···[He], or [Ne]···[Ne]. For example, in the [Ne]···[Ne]-type superatomic molecule based on a $[Au_{25}]^{9+}$ core, the occupied SAMOs follow the electron configuration $(\Sigma_{pz})^2(\Pi_{px,py})^4(\Pi^*_{px,py})^4(\Sigma^*_{pz})^2$ (Fig. 4a)[55]. Although the formal bond order in such system is regarded as zero (non-bonding), these nanoclusters are stabilized by the surrounding ligands and metal–ligand coordination frameworks.

Following pioneering work by Teo, a variety of vertex-shared superatomic molecules have been reported to date (Figs. 3b–d; see in the recent review reported by Negishi[56])[15,55–63]. In these systems, a single vertex atom is shared between two M_{13} superatoms without direct electron sharing. The formation of thiolate-protected gold nanowires has been theoretically proposed through the elongation of vertex-sharing superatomic structures, and their charge-dependent electrical conductivity has been

examined[61]. These "clusters of clusters"[57] often form cyclic structures, which may be interpreted as cyclic $[Ne]_3$[64] or $[Ne]_5$[65,66] analogues (Fig. 3e, f).

Beyond vertex-shared motifs, additional examples of non-bonding superatomic molecules have been reported. The $[Au_7]^{3+}$ cores in $Au_{20}(SR)_{16}$[67] and $Au_{22}(C\equiv CR)_{18}$[68], for instance, consist of two Au_4 (2e) superatoms that share a single gold atom (Fig. 3g). A similar structural motif has also been proposed for $Au_{22}(SR)_{18}$ based on theoretical calculations[69,70].

Another Au_4-based non-bonding configuration, $[Au_8]^{4+}$, has been observed in the cores of $Au_{24}(ER)_{18}$ (E = S, Se) nanoclusters[71–74], in which two Au_4 superatoms are arranged without any shared atoms (Fig. 3h). On the basis of various Au_4-containing polymorphs, Cheng and Yang proposed the formation of "superatomic networks" constructed of Au_4 superatomic units[75]. According to this model, the $[Au_{14}]^{6+}$ cores found in $[Au_{24}(C\equiv CR)_{14}(PPh_3)_4]^{2+}$[76], $Au_{28}(SR)_{20}$[77], and $Au_{28}(C\equiv CR)_{20}$[78] may also be interpreted as assemblies of Au_4-based superatoms.

More recently, novel types of non-bonding superatomic molecules have been reported involving bisphosphine and NHC ligands. The $[Au_{22}]^{6+}$ and $[Au_{24}]^{8+}$ cores in $[Au_{22}H_4(dppo)_6]^{2+}$ and $[Au_{24}H_3(NHC)_{14}Cl_2]^{3+}$[79–81], respectively, can be described as [Ne]···[Ne]-type superatomic molecules (Fig. 3i and j), wherein two $[Au_{11}]^{3+}$ and $[Au_{12}]^{4+}$ superatoms are combined without formal bonding but are stabilized through the coordination of chelating hydrides.

Although these systems formally possess a bond order of zero, their overall structures are stabilized by ligand coordination and surface protection. Importantly, such non-natural bonding between noble gas-type superatoms results in the emergence of new absorption bands, arising from the formation of superatomic molecular orbitals. This distinctive behavior—absent in natural atoms—is a key feature driving the development of functional materials based on superatomic molecules.

Conclusion and outlook

Superatomic molecules are assemblies of multiple superatoms connected via natural or non-natural atom-like bonding interactions, mediated through the formation of SAMOs. This review outlined the molecular and electronic structures of both superatoms and superatomic molecules. Superatomic molecules exhibiting natural atom-like bonding include representative examples of singly and multiply bonded systems, in which superatoms are connected through the sharing of multiple metal atoms. In contrast, non-natural bonding motifs encompass not only classical vertex-shared poly-icosahedral clusters but also more recently identified species such as He-type ($[Au_4]$-based) and Ne-type ($[Au_{11-13}]$-based) superatomic molecules. Molecular orbital analyses, supported by computational studies, reveal that these systems can be stabilized by chelating and surface-protecting ligands, even in cases where antibonding SAMOs are fully occupied.

To date, research in this field has primarily focused on synthesis, structural characterization, and electronic structure analysis via DFT calculations, aiming to elucidate the correlation between molecular geometry and electron configuration within the framework of the SVB model. Based on the accumulated insights, the field is now poised to transition from structural understanding to the rational design of functional materials that harness the unique characteristics of superatomic molecules.

The following perspectives are proposed for the future development of superatomic molecular materials:

1) *Superatomic molecules with natural atom-like bonding:* The bonding nature of superatomic molecules closely resembles that of conventional molecules, suggesting that similar design strategies may be applicable for the development of functional materials. Notably, symmetry-dependent electron transitions between superatomic molecular Π-orbitals have been recently observed[52], analogous to transitions in traditional π-conjugated systems. Such π-orbital resonance is a fundamental feature in controlling the functionality of a wide range of photonic and electronic applications, including luminescent materials, catalysts, and electron transport materials. Accordingly, the resonance of superatomic molecular Π-orbitals is considered a key element in the rational design of functional superatomic materials.

One essential feature associated with resonant π-systems is the emergence of aromaticity. In a seminal study, Zhu et al. reported the synthesis of a nanocluster, $[Au_{60}Se_2(PPh_3)_{10}(SePh)_{15}]^+$, containing a $[Au_{60}]^{20+}$ core composed of cyclized five icosahedral Au_{13} superatoms, each sharing one gold atom and two electrons with its neighbors via 2 superatom center-2 electron (2sc-2e) bonds (Figs. 4f and 5a)[65]. Due to the electronic shell closure within each Au_{13} unit, the $[Au_{60}]^{20+}$ core can be regarded as a cyclic $[He]_5$-type superatomic molecule. DFT-based molecular orbital analysis by Lin revealed that the five superatoms are connected via weak interactions, and although these interactions resemble non-bonding, they contribute to the overall stability of the cyclic assembly[66].

Building on this concept, Xu and Cheng proposed the design of an aromatic superatomic molecule, analogous to the cyclopentadienyl anion, by modifying the parent $[Au_{60}Se_2(PPh_3)_{10}(SePh)_{15}]^+$ nanocluster[82]. A simplified model, $[Au_{60}Se_2Cl_{15}]^+$, was employed in DFT calculations. While the parent cluster, with 40 valence electrons, corresponds to a non-aromatic cyclic $[He]_5$ system, its two-electron reduced form, $[Au_{60}Se_2Cl_{15}]^-$ (42e), as well

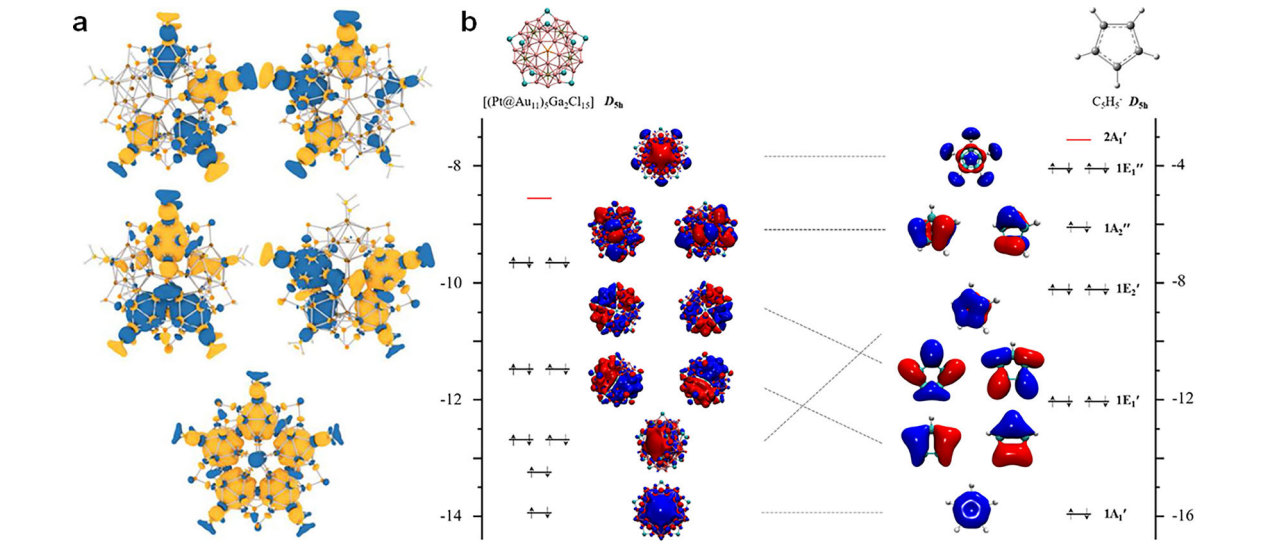

Fig. 5 Aromatic superatomic molecule. a 1S SAO-combined occupied orbitals of the $[Au_{60}Se_2(PH_3)_{10}(SeH)_{15}]+$ as a model cluster for the $[Au_{60}Se_2(PPh_3)_{10}(SePh)_{15}]^+$. **b** Comparison of the molecular orbitals for the $[(Pt@Au_{11})_5Ga_2Cl_2]$ cluster and cyclopentadienyl anion. **a**, **b** Reproduced with permission from ACS[54,69].

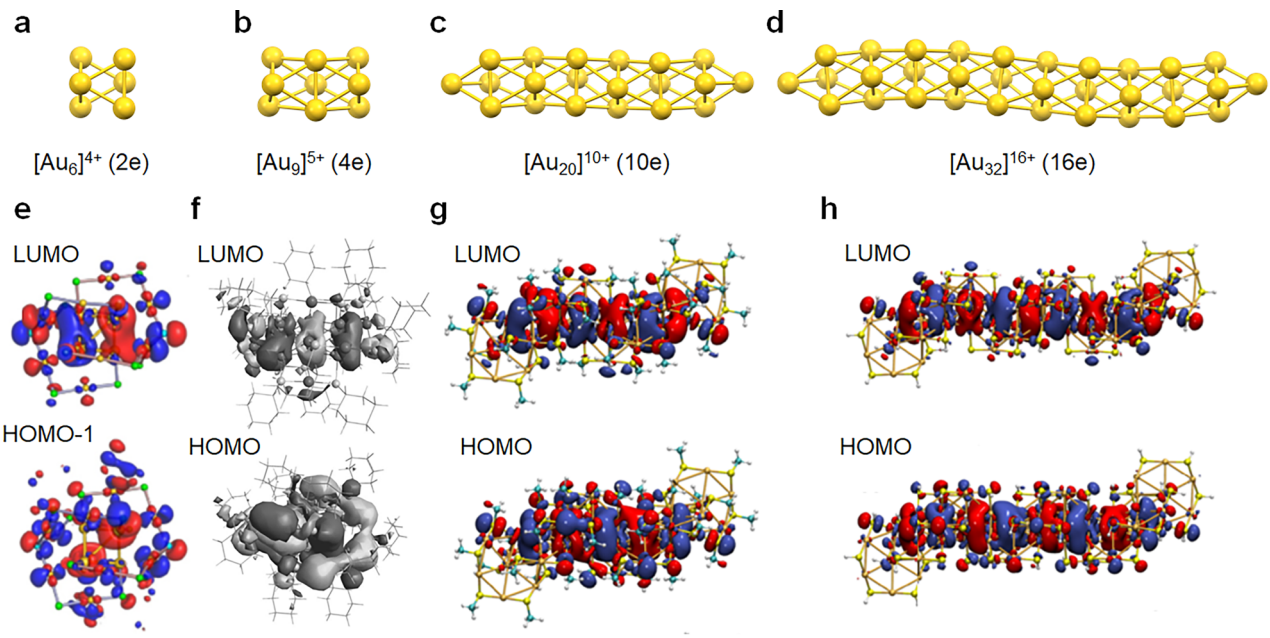

Fig. 6 Au_3-based weakly-bonding superatomic molecules. a The $[Au_6]^{4+}$ core in $Au_{18}S_2(STipb)_{12}$ composed of weakly-bonding dimer of $[Au_3]^{2+}$. **b** $[Au_9]^{5+}$ core in $Au_{18}(SCy)_{14}$ composed of weakly-bonding trimer of $[Au_3]^{+/2+}$ sequences. **c** $[Au_{20}]^{10+}$ core in $Au_{42}(PET)_{32}$ and **d** $[Au_{32}]^{16+}$ core in $Au_{60}(PET)_{44}$ composed of weakly-bonding $[Au_3]^{+/2+}$ sequences. **e**–**h** DFT-calculated Kohn–Sham orbitals of HOMO(-1) and LUMO of $Au_{18}S_2(STipb)_{12}$, $Au_{18}(SCy)_{14}$, $Au_{42}(PET)_{32}$, and $Au_{60}(PET)_{44}$. **e, f** Reproduced with permission from Wiley[70,71]. **g, h** Reproduced from PNAS[72].

as a modified version, $[(Pt@Au_{11})_5Ga_2Cl_{15}]$ (46e)—in which the central Au atoms of each icosahedral superatoms were replaced with Pt and the central-chelating Se atoms with Ga—were both predicted to exhibit aromatic character based on Hückel's $4n + 2$ rule (Fig. 5b). Furthermore, nucleus-independent chemical shift (NICS) analysis supported the aromaticity of the $[Au_{60}Se_2Cl_{15}]^-$ (42e) nanocluster.

These theoretical insights highlight the remarkable potential of superatomic molecules as candidates for super-aromatic and super-Π-delocalized materials. The ability to rationally tune aromaticity and Π-delocalization at the

superatomic level opens a new avenue for the design of advanced materials with tailored optoelectronic properties.

2) *Superatomic molecules with non-natural atom-like bonding:* Within the framework of the SVB model, numerous examples have emerged in which superatoms with closed-shell electronic configurations are combined, despite exhibiting formally non-bonding characteristics. Although these superatomic assemblies may appear non-bonded in terms of formal bond order, they frequently exhibit new absorption bands that originate from the interaction of SAOs. This unique property of superatomic molecules with non-natural atom-like bonding offers new possibilities for designing photofunctional materials that lie beyond the capabilities of conventional molecules.

A Representative example of such weakly bonded superatomic systems is the class of $[Au_3]$-based clusters. Tsukuda and co-workers reported the formation of a $[Au_6]^{4+}$ core in the $Au_{18}S_2(SR)_{12}$ nanocluster, which can be interpreted as two $[Au_3]^{2+}$ superatoms weakly interacting via 1S SAOs, despite the apparent antibonding character of the interaction (Fig. 6a, e)[83]. A structurally similar $[Au_9]^{5+}$ core was identified in $Au_{18}(SR)_{14}$[84], which consists of two $[Au_3]^{2+}$ and one $[Au_3]^{+}$ superatoms, also interacting through 1S SAOs (Fig. 6b, f).

More recently, Jin and colleagues reported a series of rod-shaped gold nanoclusters, including $Au_{42}(SR)_{32}$, $Au_{60}(SR)_{44}$, $Au_{78}(SR)_{56}$, $Au_{96}(SR)_{68}$, and $Au_{112}(SR)_{80}$, all of which incorporate repeating $[Au_3]$ units[85,86]. The cores of these nanoclusters, $[Au_{20}]^{10+}$, $[Au_{32}]^{16+}$, $[Au_{44}]^{22+}$, $[Au_{56}]^{28+}$, and $[Au_{68}]^{34+}$, respectively, can be described as a weakly bonded linear sequence of alternating $[Au_3]^{2+}$ and $[Au_3]^{+}$ superatoms, end-capped with $[Au_4]^{2+}$ units: $[Au_4]^{2+}$···2n{$[Au_3]^{2+}$···$[Au_3]^{+}$}···$[Au_4]^{2+}$ (Fig. 6c, d, g, h). These $[Au_3]$-based rod-shaped superatomic molecules exhibit intense absorption in the near infrared (NIR) region, which has never been observed in other known metal nanoclusters reported to date. Due to the weak yet coherent interactions between 1S SAOs across the superatomic chain, these structures may be interpreted as superatomic Σ-polymers, a bonding motif unique to superatomic systems. The development of such superatom Σ-polymeric architectures opens a new frontier in the design of superatom-based photofunctional materials, with promising applications in optoelectronics and photonics that are inaccessible to traditional molecular frameworks.

Acknowledgements
This work was supported by JSPS KAKENHI grant JP23K17930, The Kyoto University Foundation, ISHIZUE 2024 of Kyoto University, and Iketani Science and Technology Foundation.

Author contributions
All authors have read and approved the manuscript.

Competing interests
There are no competing interests.

Supplementary information The online version contains supplementary material available at https://doi.org/10.1038/s41427-026-00636-9.

Received: 1 July 2025 Accepted: 3 February 2026
Published online: 23 March 2026

References

1. Jin, R., Zeng, C., Zhou, M. & Chen, Y. Atomically precise colloidal metal nanoclusters and nanoparticles: fundamentals and opportunities. *Chem. Rev.* **116**, 10346–10413 (2016).
2. Kawawaki, T. et al. Thiolate-protected metal nanoclusters: recent development in synthesis, understanding of reaction, and application in energy and environmental field. *Small* **17**, 2005328 (2021).
3. Bose, P., Kumaranchira Ramankutty, K., Chakraborty, P., Khatun, E. & Pradeep, T. A concise guide to chemical reactions of atomically precise noble metal nanoclusters. *Nanoscale* **16**, 1446–1470 (2024).
4. Omoda, T., Takano, S. & Tsukuda, T. Toward controlling the electronic structures of chemically modified superatoms of gold and silver. *Small* **17**, 2001439 (2021).
5. Saito, Y., Murata, C., Sugiuchi, M., Shichibu, Y. & Konishi, K. Ligand-coordinated metal clusters in condensed states: self-assemblies, crystals, and covalent networks. *Coord. Chem. Rev.* **470**, 214713 (2022).
6. Li, Y., Zhou, M. & Jin, R. Programmable metal nanoclusters with atomic precision. *Adv. Mater.* **33**, 2006591 (2021).
7. Jin, R., Li, G., Sharma, S., Li, Y. & Du, X. Toward active-site tailoring in heterogeneous catalysis by atomically precise metal nanoclusters with crystallographic structures. *Chem. Rev.* **121**, 567–648 (2021).
8. Du, Y., Sheng, H., Astruc, D. & Zhu, M. Atomically precise noble metal nanoclusters as efficient catalysts: a bridge between structure and properties. *Chem. Rev.* **120**, 526–622 (2020).
9. Li, S., Li, N.-N., Dong, X.-Y., Zang, S.-Q. & Mak, T. C. W. Chemical flexibility of atomically precise metal clusters. *Chem. Rev.* **124**, 7262–7378 (2024).
10. Lei, Z., Wan, X.-K., Yuan, S.-F., Wang, J.-Q. & Wang, Q.-M. Alkynyl-protected gold and gold–silver nanoclusters. *Dalton Trans.* **46**, 3427–3434 (2017).
11. Yuan, S., Liu, W., Liu, C., Guan, Z. & Wang, Q. Nitrogen donor protection for atomically precise metal nanoclusters. *Chem. Eur. J.* **28**, e202104445 (2022).
12. Albright, E. L. et al. *N* -heterocyclic carbene-stabilized atomically precise metal nanoclusters. *J. Am. Chem. Soc.* **146**, 5759–5780 (2024).
13. de Heer, W. A. The physics of simple metal clusters: experimental aspects and simple models. *Rev. Mod. Phys.* **65**, 611–676 (1993).
14. Walter, M. et al. A unified view of ligand-protected gold clusters as superatom complexes. *Proc. Natl. Acad. Sci. USA* **105**, 9157–9162 (2008).
15. Teo, B. K. & Zhang, H. Polyicosahedricity: icosahedron to icosahedron of icosahedra growth pathway for bimetallic (Au–Ag) and trimetallic (Au–Ag–M; M = Pt, Pd, Ni) superclusters; synthetic strategies, site preference, and stereochemical principles. *Coord. Chem. Rev.* **143**, 611–636 (1995).
16. Cheng, L., Ren, C., Zhang, X. & Yang, J. New insight into the electronic shell of $Au_{38}(SR)_{24}$: a superatomic molecule. *Nanoscale* **5**, 1475 (2013).
17. Yuan, Y., Cheng, L. & Yang, J. Electronic stability of phosphine-protected Au_{20} nanocluster: superatomic bonding. *J. Phys. Chem. C* **117**, 13276–13282 (2013).
18. Cheng, L. & Yang, J. Communication: new insight into electronic shells of metal clusters: Analogues of simple molecules. *J. Chem. Phys.* **138**, 141101 (2013).
19. Taylor, K. J., Pettiette-Hall, C. L., Cheshnovsky, O. & Smalley, R. E. Ultraviolet photoelectron spectra of coinage metal clusters. *J. Chem. Phys.* **96**, 3319–3329 (1992).
20. Ueda, K. et al. Accelerated catalysis of atomically precise thiolate-protected gold nanocluster by supramolecular ligand engineering. *ACS Catal.* **15**, 12260–12268 (2025).
21. Isozaki, K., Iseri, K., Saito, R., Ueda, K. & Nakamura, M. Dual catalysis of gold nanoclusters: photocatalytic cross-dehydrogenative coupling by cooperation of superatomic core and molecularly modified staples. *Angew. Chem. Int. Ed.* **63**, e202312135 (2024).

22. Isozaki, K. et al. Gold nanocluster functionalized with peptide dendron thiolates: acceleration of the photocatalytic oxidation of an amino alcohol in a supramolecular reaction field. *ACS Catal.* **11**, 13180–13187 (2021).
23. Muñoz-Castro, A. On the ligand–core interaction in ligand-protected gold superatoms. Insights from $Au_{25}(XR)_{18}$ (X = S, Se, Te) *via* relativistic DFT calculations. *Phys. Chem. Chem. Phys.* **21**, 13022–13029 (2019).
24. Strienz, M. et al. $Au_{147}(SPh)_{30}(PPh_3)_{12}$: a geometrically closed, but electronically open triple-shell icosahedral gold cluster and its geometrically open counterpart. *Angew. Chem. Int. Ed.* **64**, e202500586 (2025).
25. He, W.-M. et al. Filling the gaps in icosahedral superatomic metal clusters. *Nat. Sci. Rev.* **11**, nwae174 (2024).
26. Yan, J. et al. Asymmetric synthesis of chiral bimetallic $[Ag_{28}Cu_{12}(SR)_{24}]^{4-}$ nanoclusters via Ion pairing. *J. Am. Chem. Soc.* **138**, 12751–12754 (2016).
27. Jia, T. et al. Eight-electron superatomic Cu_{31} nanocluster with chiral Kernel and NIR-II emission. *J. Am. Chem. Soc.* **145**, 10355–10363 (2023).
28. Qian, H., Eckenhoff, W. T., Zhu, Y., Pintauer, T. & Jin, R. Total structure determination of thiolate-protected Au_{38} nanoparticles. *J. Am. Chem. Soc.* **132**, 8280–8281 (2010).
29. Chaki, N. K., Negishi, Y., Tsunoyama, H., Shichibu, Y. & Tsukuda, T. Ubiquitous 8 and 29 kDa gold:alkanethiolate cluster compounds: mass-spectrometric determination of molecular formulas and structural implications. *J. Am. Chem. Soc.* **130**, 8608–8610 (2008).
30. Rodríguez-Kessler, P. L. & Muñoz-Castro, A. Intermediate intercluster bond orders. electronic communication in $Au_{38}(SR)_{24}$ superatomic molecules. *Chem. Phys. Chem* **25**, e202400183 (2024).
31. Liu, X. et al. Asymmetrically doping a platinum atom into a Au_{38} nanocluster for changing the electron configuration and reactivity in electrocatalysis. *Angew. Chem. Int. Ed.* **61**, e202207685 (2022).
32. Pollitt, S. et al. The dynamic structure of $Au_{38}(SR)_{24}$ nanoclusters supported on CeO_2 upon pretreatment and CO oxidation. *ACS Catal* **10**, 6144–6148 (2020).
33. Zhao, J. et al. Reversible control of chemoselectivity in $Au_{38}(SR)_{24}$ nanocluster-catalyzed transfer hydrogenation of nitrobenzaldehyde derivatives. *J. Phys. Chem. Lett.* **9**, 7173–7179 (2018).
34. Li, Q., Das, A., Wang, S., Chen, Y. & Jin, R. Highly efficient three-component coupling reaction catalysed by atomically precise ligand-protected $Au_{38}(SC_2H_4Ph)_{24}$ nanoclusters. *Chem. Commun.* **52**, 14298–14301 (2016).
35. Zhang, B. et al. Modulation of active sites in supported $Au_{38}(SC_2H_4Ph)_{24}$ cluster catalysts: effect of atmosphere and support material. *J. Phys. Chem. C* **119**, 11193–11199 (2015).
36. Knoppe, S. & Bürgi, T. Chirality in thiolate-protected gold clusters. *Acc. Chem. Res.* **47**, 1318–1326 (2014).
37. Barrabés, N., Zhang, B. & Bürgi, T. Racemization of chiral $Pd_2Au_{36}(SC_2H_4Ph)_{24}$: doping increases the flexibility of the cluster surface. *J. Am. Chem. Soc.* **136**, 14361–14364 (2014).
38. Dolamic, I., Knoppe, S., Dass, A. & Bürgi, T. First enantioseparation and circular dichroism spectra of Au_{38} clusters protected by achiral ligands. *Nat. Commun.* **3**, 798 (2012).
39. Zou, X. et al. Multi-ligand-directed synthesis of chiral silver nanoclusters. *Nanoscale* **9**, 16800–16805 (2017).
40. Zhou, M. et al. Synthesis, structural characterization, and electronic structure analysis of F_2-type superatomic molecules. *Inorg. Chem.* **63**, 23722–23779 (2024).
41. Nishigaki, J. et al. A twisted bi-icosahedral Au_{25} cluster enclosed by bulky arenethiolates. *Chem. Commun.* **50**, 839–841 (2014).
42. Matsuo, S., Yamazoe, S., Goh, J.-Q., Akola, J. & Tsukuda, T. The electrooxidation-induced structural changes of gold di-superatomic molecules: Au_{23} vs. Au_{25}. *Phys. Chem. Chem. Phys.* **18**, 4822–4827 (2016).
43. Akazawa, K., Ito, S., Hamasaki, Y., Koyasu, K. & Tsukuda, T. HOMO–LUMO gap of $[Au_{38}(SC_2H_4Ph)_{24}]^0$ estimated by photoelectron spectroscopy on Its MALDI-generated anion. *J. Phys. Chem. A* **129**, 6043–6048 (2025).
44. Qian, H., Barry, E., Zhu, Y. & Jin, R. Doping 25-atom and 38-atom gold nanoclusters with palladium. *Acta Phys. Chem. Sin.* **27**, 513–519 (2011).
45. Negishi, Y., Igarashi, K., Munakata, K., Ohgake, W. & Nobusada, K. Palladium doping of magic gold cluster $Au_{38}(SC_2H_4Ph)_{24}$: formation of $Pd_2Au_{36}(SC_2H_4Ph)_{24}$ with higher stability than $Au_{38}(SC_2H_4$ $Ph)_{24}$. *Chem. Commun.* **48**, 660–662 (2012).
46. Kim, M. et al. Dopant-dependent electronic structures observed for $M_2Au_{36}(SC_6H_{13})_{24}$ Clusters (M = Pt, Pd). *J. Phys. Chem. Lett.* **9**, 982–989 (2018).
47. Muñoz-Castro, A. Single, double, and triple intercluster bonds: analyses of $M_2Au_{36}(SR)_{24}$ (M = Au, Pd, Pt) as 14-, 12- and 10-ve superatomic molecules. *Chem. Commun.* **55**, 7307–7310 (2019).
48. Ito, E., Takano, S., Nakamura, T. & Tsukuda, T. Controlled dimerization and bonding scheme of Icosahedral $M@Au_{12}$ (M=Pd, Pt) superatoms. *Angew. Chem. Int. Ed.* **60**, 645–649 (2021).
49. Ito, E., Ito, S., Takano, S., Nakamura, T. & Tsukuda, T. Supervalence bonding in Bi-icosahedral Cores of $[M_1Au_{37}(SC_2H_4Ph)_{24}]^-$ (M = Pd and Pt): fusion-mediated synthesis and anion photoelectron spectroscopy. *JACS Au* **2**, 2627–2634 (2022).
50. Xu, C., Zhou, Y., Shi, L. & Cheng, L. Superatomic three-center bond in a Tri-Icosahedral $Au_{36}Ag_2(SR)_{18}$ cluster: analogue of 3c-2e bond in molecules. *J. Phys. Chem. Lett.* **13**, 10147–10152 (2022).
51. Li, Y. et al. Hydrogen evolution electrocatalyst design: turning inert gold into active catalyst by atomically precise nanochemistry. *J. Am. Chem. Soc.* **143**, 11102–11108 (2021).
52. Saito, R., Isozaki, K., Mizuhata, Y. & Nakamura, M. Synthesis of N_2-type superatomic molecules. *J. Am. Chem. Soc.* **146**, 20930–20936 (2024).
53. Yuan, Q., Gao, J., Zheng, Y., Xu, C. & Cheng, L. Assembling gold icosahedrons to superatomic molecules mimicking the bonding rules in molecules. *Inorg. Chem.* **64**, 452–459 (2025).
54. Xu, C. et al. Tri- and tetra-superatomic molecules in ligand-protected face-fused icosahedral $(M@Au_{12})_n$ (M = Au, Pt, Ir, and Os, and n = 3 and 4) clusters. *J. Phys. Chem. Lett.* **13**, 1931–1939 (2022).
55. Shen, H. et al. Highly robust but surface-active: an N-heterocyclic carbene-stabilized Au_{25} nanocluster. *Angew. Chem. Int. Ed.* **58**, 17731–17735 (2019).
56. Niihori, Y., Miyajima, S., Ikeda, A., Kosaka, T. & Negishi, Y. Vertex-shared linear superatomic molecules: stepping stones to novel materials composed of noble metal clusters. *Small Sci.* **3**, 2300024 (2023).
57. Teo, B. K. & Keating, K. Novel triicosahedral structure of the largest metal alloy cluster: $[(Ph_3P)_{12}Au_{13}Ag_{12}Cl_6]^{m+}$. *J. Am. Chem. Soc.* **106**, 2224–2226 (1984).
58. Nobusada, K. & Iwasa, T. Oligomeric gold clusters with vertex-sharing bi- and triicosahedral structures. *J. Phys. Chem. C* **111**, 14279–14282 (2007).
59. Shichibu, Y. et al. Biicosahedral gold clusters $[Au_{25}(PPh_3)_{10}(SC_nH_{2n+1})_5Cl_2]^{2+}$ (n = 2−18): a stepping stone to cluster-assembled materials. *J. Phys. Chem. C* **111**, 7845–7847 (2007).
60. Jin, R. et al. Tri-icosahedral gold nanocluster $[Au_{37}(PPh_3)_{10}(SC_2H_4Ph)_{10}X_2]^+$: linear assembly of icosahedral building blocks. *ACS Nano* **9**, 8530–8536 (2015).
61. Jiang, D., Nobusada, K., Luo, W. & Whetten, R. L. Thiolated gold nanowires: metallic *versus* Semiconducting. *ACS Nano* **3**, 2351–2357 (2009).
62. Zhou, M. et al. Electron localization in rod-shaped triicosahedral gold nanocluster. *Proc. Natl. Acad. Sci. USA* **114**, E4697–E4705 (2017).
63. Yuan, S.-F. et al. Rod-shaped silver supercluster unveiling strong electron coupling between substituent icosahedral units. *J. Am. Chem. Soc.* **143**, 12261–12267 (2021).
64. Teo, B. K., Zhang, H. & Shi, X. Cluster of clusters: a modular approach to large metal clusters. Structural characterization of a 38-atom cluster $[(p\text{-}Tol_3\text{-}P)_{12}Au_{18}Ag_{20}Cl_{14}]$ based on vertex-sharing triicosahedra. *J. Am. Chem. Soc.* **112**, 8552–8562 (1990).
65. Song, Y. et al. The magic Au_{60} nanocluster: a new cluster-assembled material with five Au_{13} building blocks. *Angew. Chem. Int. Ed* **54**, 8430–8434 (2015).
66. Sheong, F. K., Zhang, J.-X. & Lin, Z. An $[Au_{13}]^{5+}$ approach to the study of gold nanoclusters. *Inorg. Chem.* **55**, 11348–11353 (2016).
67. Zeng, C., Liu, C., Chen, Y., Rosi, N. L. & Jin, R. Gold–thiolate ring as a protecting motif in the $Au_{20}(SR)_{16}$ nanocluster and implications. *J. Am. Chem. Soc.* **136**, 11922–11925 (2014).
68. Ito, S., Takano, S. & Tsukuda, T. Alkynyl-protected $Au_{22}(C{\equiv}CR)_{18}$ clusters featuring new interfacial motifs and R-dependent photoluminescence. *J. Phys. Chem. Lett.* **10**, 6892–6896 (2019).
69. Pei, Y., Tang, J., Tang, X., Huang, Y. & Zeng, X. C. New structure model of $Au_{22}(SR)_{18}$: bitetrahederon golden Kernel enclosed by $[Au_6(SR)_6]$ Au(I) complex. *J. Phys. Chem. Lett.* **6**, 1390–1395 (2015).
70. Yu, Y. et al. Identification of a highly luminescent $Au_{22}(SG)_{18}$ nanocluster. *J. Am. Chem. Soc.* **136**, 1246–1249 (2014).
71. Takagi, N. et al. How can we understand Au_8 cores and entangled ligands of selenolate- and thiolate-protected gold nanoclusters $Au_{24}(ER)_{20}$ and $Au_{20}(ER)_{16}$ (E = Se, S; R = Ph, Me)? a theoretical study. *J. Am. Chem. Soc.* **137**, 8593–8602 (2015).
72. Song, Y. et al. Crystal structure of selenolate-protected $Au_{24}(SeR)_{20}$ nanocluster. *J. Am. Chem. Soc.* **136**, 2963–2965 (2014).
73. Pei, Y. et al. Interlocked catenane-like structure predicted in $Au_{24}(SR)_{20}$: implication to structural evolution of thiolated gold clusters from homoleptic gold(I) thiolates to core-stacked nanoparticles. *J. Am. Chem. Soc.* **134**, 3015–3024 (2012).

74. Zhu, M., Qian, H. & Jin, R. Thiolate-protected $Au_{24}(SC_2H_4Ph)_{20}$ nanoclusters: Superatoms or not? *J. Phys. Chem. Lett.* **1**, 1003–1007 (2010).
75. Cheng, L., Yuan, Y., Zhang, X. & Yang, J. Superatom networks in thiolate-protected gold nanoparticles. *Angew. Chem. Int. Ed.* **52**, 9035–9039 (2013).
76. Wan, X. et al. A near-infrared-emissive alkynyl-protected Au_{24} nanocluster. *Angew. Chem. Int. Ed* **54**, 9683–9686 (2015).
77. Zeng, C., Li, T., Das, A., Rosi, N. L. & Jin, R. Chiral structure of thiolate-protected 28-gold-atom nanocluster determined by X-ray crystallography. *J. Am. Chem. Soc.* **135**, 10011–10013 (2013).
78. Tang, S. et al. Aromatic alkyne-protected Au_{28} nanoclusters for electrocatalytic ethanol oxidation. *Catal. Sci. Technol.* **13**, 5821–5824 (2023).
79. Chen, J., Zhang, Q.-F., Bonaccorso, T. A., Williard, P. G. & Wang, L.-S. Controlling gold nanoclusters by diphospine ligands. *J. Am. Chem. Soc.* **136**, 92–95 (2014).
80. Dong, J., Gao, Z., Zhang, Q. & Wang, L. The Synthesis, Bonding, and Transformation of a Ligand-Protected Gold Nanohydride Cluster. *Angew. Chem. Int. Ed.* **60**, 2424–2430 (2021).
81. Kulkarni, V. K. et al. N-heterocyclic carbene-stabilized hydrido Au_{24} nanoclusters: synthesis, structure, and electrocatalytic reduction of CO_2. *J. Am. Chem. Soc.* **144**, 9000–9006 (2022).
82. Gao, J., Zhou, Y., Xu, C. & Cheng, L. Superatomic aromaticity in cyclic superatomic molecules: ligand-protected penta-icosahedral $[M@Au_{11}]_5$ (M = Au, Pt) clusters. *J. Phys. Chem. A* **128**, 2982–2988 (2024).
83. Shigeta, T., Takano, S. & Tsukuda, T. A face-to-face dimer of Au_3 superatoms supported by interlocked tridentate scaffolds formed in $Au_{18}S_2(SR)_{12}$. *Angew. Chem. Int. Ed.* **61**, e202113275 (2022).
84. Das, A. et al. Structure determination of $[Au_{18}(SR)_{14}]$. *Angew. Chem. Int. Ed.* **54**, 3140–3144 (2015).
85. Luo, L. et al. Three-atom-wide gold quantum rods with periodic elongation and strongly polarized excitons. *Proc. Natl. Acad. Sci. USA.* **121**, e2318537121 (2024).
86. Li, Y. et al. Atomically precise Au_{42} nanorods with longitudinal excitons for an intense photothermal effect. *J. Am. Chem. Soc.* **144**, 12381–12389 (2022).